

Training neural networks with structured noise improves classification and generalization

Marco Benedetti^{1,*} and Enrico Ventura^{1,2,*}

¹*Dipartimento di Fisica, Sapienza Università di Roma, P.le A. Moro 2, 00185 Roma, Italy*

²*Laboratoire de Physique de l'Ecole Normale Supérieure, ENS, Université PSL, F-75005 Paris, France*

The beneficial role of noise in learning is nowadays a consolidated concept in the field of artificial neural networks. The training-with-noise algorithm proposed by Gardner and collaborators is an emblematic example of a noise injection procedure in recurrent networks. We show how adding structure into noisy training data can substantially improve memory performance, allowing to approach perfect classification and maximal basins of attraction. We also prove that the so-called unlearning rule coincides with the training-with-noise algorithm when noise is maximal and data are fixed points of the network dynamics. Moreover, a sampling scheme for optimal noisy data is proposed and implemented to outperform both the training-with-noise and the unlearning procedures.

I. INTRODUCTION

Consider a fully connected network of N binary variables $\{S_i = \pm 1\}$, $i \in [1, \dots, N]$, linked by couplings J_{ij} . The network is endowed with a dynamics

$$S_i(t+1) = \text{sign} \left(\sum_{j=1}^N J_{ij} S_j(t) \right), \quad i = 1, \dots, N \quad (1)$$

which can be run either in parallel (i.e. *synchronously*) or in series (i.e. *asynchronously*) over the i indices. We will mainly concentrate on asynchronous dynamics, in which case eq. (1) can only converge to fixed points, when they exist. This kind of network can be used as an associative memory device, namely for reconstructing a number p of configurations $\{\xi_i^\mu\} = \pm 1$, $\mu \in [1, \dots, p]$, called *memories*, when initialized into a configuration similar enough to one of them. In this work, we will concentrate on i.i.d. memories, generated with a probability $P(\xi_i^\mu = \pm 1) = 1/2$. The number of memories is extensive $p = \alpha N$, where α is called *load* of the network. The network is considered to perform well if such asymptotic states are similar enough to the memories. Whether this is the case, depends on the choice of the coupling matrix J . To give an example, Hebb's (or Hebbian) learning prescription [1, 2]

$$J_{ij}^H = \frac{1}{N} \sum_{\mu=1}^p \xi_i^\mu \xi_j^\mu \quad (2)$$

is a rudimentary yet effective rule that allows to retrieve memories up to a critical capacity $\alpha_c^H \sim 0.14$ [3]. Notably, when $\alpha < \alpha_c^H$ memories are not perfectly recalled, but only reproduced with a small number of errors. Several techniques have been developed to build better performing coupling matrices, i.e. to reduce the retrieval error and increase the critical capacity as well as the size

of the basins of attraction to which the memories belong. Three significant examples are the unlearning algorithm [4–9], the linear perceptron algorithms [10–12], and the training-with-noise algorithm [13]. All these procedures rely on iteratively modifying the couplings on the basis of an initial choice of the couplings and a set of training data presented to the network. Each step of the unlearning algorithm does not explicitly use the memories, and only exploits the information encoded in Hebb's rule. On the other hand, the linear perceptron is trained with the pure memories until they become attractors of the network dynamics. In analogy with a noisy linear perceptron, Gardner and collaborators proposed the training-with-noise algorithm, managing to increase the size of the basins of attraction while conserving a rather high accuracy in the memory retrieval. In this context, *noise* is defined as the degree of similarity between training data and memories: the higher the noise, the more the presented data differ from the memories.

The main goal of this work is to show that, the training-with-noise algorithm can be considerably improved, when training data contain internal dependencies, that we call *structure*. Specifically, in case of maximal noise, we derive a condition to be satisfied by the structure to drive learning towards the best memory performance. We also show that not all initial conditions are supplied with the best training data, and that previous Hebbian learning already provides for a good noise structure. Remarkably, we have found that the unlearning rule emerges from training-with-noise in the particular case of maximal noise and training data chosen to be fixed points of (1). We also developed an effective sampler device for optimal noisy training data that can be used to reach higher critical capacities while preserving rather large basins of attraction of the memories.

The paper is organized as follows: in Sec. II we define some measures for the network performance, in particular the concepts of classification and generalization. In Sec. III and Sec. IV we describe the unlearning and the training-with-noise algorithms and their effects on the neural network. Successively, in Sec. V the role of noise structure in training data is extensively discussed,

* The two authors contributed equally

with a particular attention on the cases of maximal and moderate noise injection. Eventually in Sec. VI we use insights from the previous sections to devise a performing sampling algorithm for training data.

II. NETWORK PERFORMANCE

In this section we describe how to benchmark the neural network performance, specifically in terms of the dynamic stability achieved by the memory vectors and the ability of the system to retrieve blurry examples of the latter.

We define *classification* as the capability to perfectly retrieve each memory when the dynamics is initialized to the memory itself. The fraction among all pN units ξ_i^μ that are stable according to one step of the dynamics (1) will be called n_{SAT} , in analogy with the celebrated perceptron optimization problem [10, 12]. Classification is reached when $n_{SAT} = 1$.

We define *generalization* as the capability to retrieve the memory, or a configuration that is strongly related to it, by initializing the dynamics on a noise-corrupted version of the memory. This property of the neural network is related to the size of the basins of attraction to which the memories belong, and does not imply $n_{SAT} = 1$. A good measure of the performance in this sense is the *retrieval map*

$$m_f(m_0) := \overline{\left\langle \frac{1}{N} \sum_{i=1}^N \xi_i^\nu S_i^\nu(\infty) \right\rangle}. \quad (3)$$

Here, $\vec{S}^\nu(\infty)$ is the stable fixed point reached by the network, when it exists, when the dynamics is initialized to a configuration $\vec{S}^\nu(0)$ having overlap m_0 with a given memory $\vec{\xi}^\nu$. The symbol $\overline{\cdot}$ denotes the average over different realizations of the memories and $\langle \cdot \rangle$ the average over different realizations of $\vec{S}^\nu(0)$. In the classification regime, one obtains $m_f = 1$ when $m_0 = 1$. The analytical computation of the retrieval map might be challenging for some networks. Hence one can introduce another indicative observable for the generalization, i.e. the *one-step retrieval map* $m_1(m_0)$ [14], defined by applying a single step of *synchronous* dynamics (1):

$$m_1(m_0) := \overline{\frac{1}{N} \sum_{i=1}^N \left\langle \xi_i^\nu \operatorname{sign} \left(\sum_{j=1}^N J_{ij} S_j^\nu(0) \right) \right\rangle}, \quad (4)$$

This work is devoted to exploring the characteristics of the training process leading to classification and good generalization.

III. UNLEARNING

Inspired by the brain functioning during REM sleep [5], the unlearning algorithm [4–8] is a training procedure

leading to classification and good generalization in a symmetric neural network. This section contains an introduction to the algorithm as well as a description of the gained performance in terms of classification and generalization.

Training starts by initializing the connectivity matrix according to Hebb's rule eq. (2) (i.e. $J^0 = J^H$). Then, the following procedure is iterated at each step d :

1. Initialize of the network dynamics (1) on a random neural state.
2. Run the asynchronous dynamics until convergence to a stable fixed point $\vec{S}^{(d)}$.
3. Update couplings according to:

$$\delta J_{ij}^{(d)} = -\frac{\lambda}{N} S_i^{(d)} S_j^{(d)} \quad J_{ii} = 0 \quad \forall i. \quad (5)$$

This algorithm was first introduced to prune the landscape of attractors from proliferating spurious states, i.e. fixed points of (1) not coinciding with the memories [15, 16]. Such spurious states are only weakly correlated with the memories. Even though this pruning action leads to the full stabilization of the memories, the exact mechanism behind this effect is not completely understood. The analysis in [8] gives deeper insights in both the classification and generalization capabilities of a network trained with unlearning.

A. Classification

The classification property is achieved running the algorithm when $\alpha \leq \alpha_c^U$ with $\alpha_c^U \simeq 0.6$. To quantify the classification performance of the network, one can track numerically the observable

$$\Delta_{\min} = \overline{\min_{i,\mu} (\Delta_i^\mu)}, \quad (6)$$

where the *stability* Δ_i^μ is defined by

$$\Delta_i^\mu = \frac{\xi_i^\mu}{\sqrt{N} \sigma_i} \sum_{j=1}^N J_{ij} \xi_j^\mu, \quad \sigma_i = \sqrt{\sum_{j=1}^N J_{ij}^2 / N}. \quad (7)$$

As soon as $\Delta_{\min} > 0$, memories become fixed points of the dynamics [10]. Fig. 1 reports the evolution of Δ_{\min} as a function of the number of performed updates of J , for $\alpha = 0.3$. The amount of iterations $d = d_{in}$ (indicated with a red circle) marks when Δ_{\min} crosses 0. At this point, all the memories are fixed points of the dynamics. Other two points, $d = (d_{top}, d_{fin})$ are reported in the plot, even though [8] has proved d_{in} to show the best generalization performance in the large N limit. The scaling of $(d_{in}, d_{top}, d_{fin})$ is also described in [8]. The progressive decay of Δ_{\min} , that becomes negative again after $d = d_{fin}$, is due to the vanishing of the first two moments of the couplings.

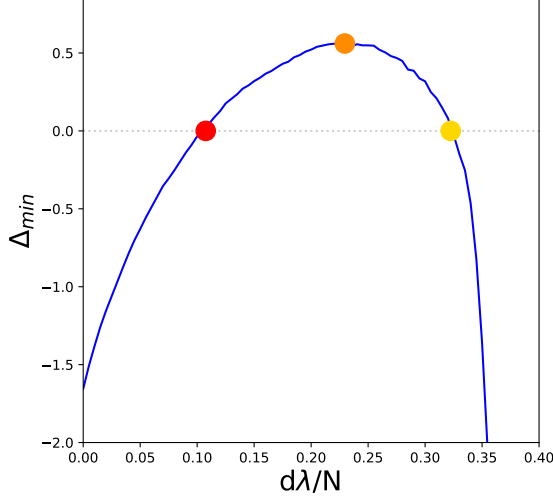


FIG. 1: The minimum stability Δ_{\min} as a function of the normalized algorithm time. The threshold $\Delta = 0$ is indicated with the gray dotted line. Three relevant amount of iterations are indicated by the colored circles: $d = d_{in}$ in red, $d = d_{top}$ in orange, $d = d_{fin}$ in yellow. All measures are averaged over 50 realizations of the network. Choice of the parameters: $N = 100$, $\alpha = 0.3$, $\lambda = 10^{-2}$.

B. Generalization

The unlearning algorithm creates large basins of attraction around the memories, when $\alpha < \alpha_c^U$. Fig. 2 reports the retrieval map for $N = 100$ and $\alpha = 0.3$. The curves relative to the SVM and unlearning at $d = d_{in}$ coincide. This observation is coherent with estimates for the large N limit performed in [8]. The SVM is trained with no symmetry constraints, though it superimposes with the symmetric version discussed in [8, 11, 17]: this is probably due to the high degree of symmetry displayed by SVMs. Fig. 2 also shows that curves for $d = d_{in}$ and $d = d_{top}$ do overlap significantly. This is certainly due to finite size effects, since [8] clearly shows the basins to progressively deteriorate, in the large N limit, along the interval $d \in [d_{in}, d_{fin}]$.

One open issue is why the optimum is found when $\Delta_{\min} = 0$ (i.e. $d = d_{in}$) and not when Δ_{\min} is maximum (i.e. $d = d_{top}$). A second question regards why unlearning, and the choice of using fixed points as training data, should lead to maximally large basins of attraction.

IV. TRAINING WITH NOISE

The concept of learning from noisy examples, introduced for the first time in [18], is at the basis of Gardner and co-workers work [13], a pioneering attempt to in-

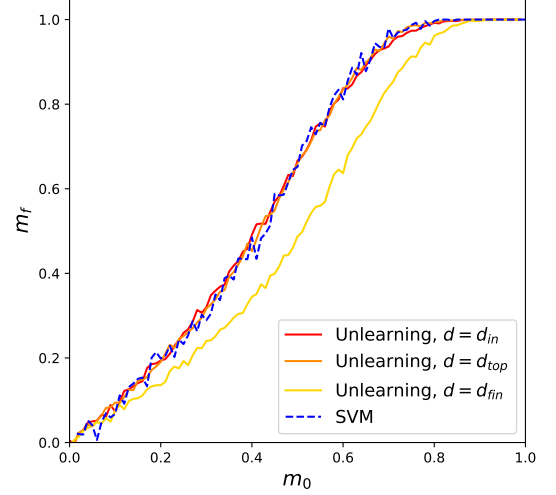


FIG. 2: Retrieval map $m_f(m_0)$ for a SVM and the unlearning algorithm at the three relevant steps indicated in fig. 1. All measures are averaged over 10 realizations of the network. Choice of the parameters: $N = 100$, $\alpha = 0.3$, $\lambda = 10^{-2}$ for unlearning and $\lambda = 1$ for the SVM.

crease and control generalization through the introduction of noise during the training phase of recurrent neural networks. Here, we report the algorithm and characterize, for the first time, its performance over fully connected neural networks.

The training-with-noise algorithm [13] consists in starting from any initial coupling matrix J_{ij}^0 with null entries on the diagonal, and updating recursively the couplings according to

$$\delta J_{ij}^{(d)} = \frac{\lambda}{N} \epsilon_i^{\mu_d} \xi_i^{\mu_d} S_j^{\mu_d}, \quad \delta J_{ii}^{(d)} = 0 \quad \forall i, \quad (8)$$

where λ is a small learning rate, $\mu_d \in [1, \dots, p]$ is a randomly chosen memory index and the mask $\epsilon_i^{\mu_d}$ is defined as

$$\epsilon_i^{\mu_d} = \frac{1}{2} \left(1 - \text{sign} \left(\xi_i^{\mu_d} \sum_{k=1}^N J_{ik} S_k^{\mu_d} \right) \right). \quad (9)$$

In this setting, \tilde{S}^{μ_d} is a noisy memory, generated according to

$$P(S_i^{\mu_d} = x) = \frac{(1 + m_t)}{2} \delta(x - \xi_i^{\mu_d}) + \frac{(1 - m_t)}{2} \delta(x + \xi_i^{\mu_d}). \quad (10)$$

The *training overlap* m_t is a control parameter for the level of *noise* injected during training, corresponding to the expected overlap between \tilde{S}^{μ_d} and ξ^{μ_d} , i.e.

$$m_t = \frac{1}{N} \sum_{j=1}^N \xi_j^{\mu_d} S_j^{\mu_d} + O\left(\frac{1}{\sqrt{N}}\right). \quad (11)$$

Each noisy configuration can be expressed in terms of a vector of *noise units* $\tilde{\chi}$, such that

$$S_i^{\mu_d} = \chi_i^{\mu_d} \xi_i^{\mu_d}. \quad (12)$$

In this setting, noise units are i.i.d variables, distributed according to

$$P(\chi_i^{\mu_d} = x) = \frac{(1+m_t)}{2} \delta(x-1) + \frac{(1-m_t)}{2} \delta(x+1). \quad (13)$$

The algorithm would converge when every configuration with overlap m_t with a memory generates on each site a local field aligned with the memory itself. Let us define the function

$$\mathcal{L}(m, J) = -\frac{1}{\alpha N^2} \sum_{i,\mu} \text{erf} \left(\frac{m \Delta_i^\mu}{\sqrt{2(1-m^2)}} \right). \quad (14)$$

Assuming that stabilities are self-averaging quantities, it can be proven that $-\mathcal{L}(m = m_0, J)$ tends to $m_1(m_0)$ when $N \rightarrow \infty$ [14, 19]. Each step of the training procedure (8) leads to a reduction of $\mathcal{L}(m, J)$, for any value of m and m_t . In fact, considering a small variation of the stabilities induced by the algorithm update

$$\Delta_i^\mu \rightarrow \Delta_i^\mu + \delta \Delta_i^\mu,$$

and performing a Taylor expansion of (14) at first order in $O(N^{-1/2})$, one obtains (see Appendix A 1)

$$\mathcal{L}' = \mathcal{L} + \sum_{i=1}^N \delta \mathcal{L}_i \quad (15)$$

where

$$\delta \mathcal{L}_i = -\frac{\epsilon_i^{\mu_d} \lambda}{\alpha \sigma_i N^{5/2}} \frac{\sqrt{2} m \cdot m_t}{\sqrt{\pi(1-m^2)}} \exp \left(-\frac{m^2 \Delta_i^{\mu_d^2}}{2(1-m^2)} \right). \quad (16)$$

Hence, $\delta \mathcal{L}_i$ is strictly non-positive when $\frac{\lambda}{N}$ is small, so that the Taylor expansion is justified. Now, the couplings' variance σ_i (see eq. (7)) is a variable quantity over time, and numerics suggest it is slowly decreasing. As a result, the expansion performed to determine the variation of \mathcal{L} might not be appropriate after a certain number of steps, leading to a non-monotonic trend of the function. This inconvenience can be overcome by transforming the learning rate λ into $\lambda_i = \lambda \cdot \sigma_i$ at each iteration.

Wong and Sherrington [20, 21] propose an elegant analysis of a network designed to optimize $\mathcal{L}(m, J)$, i.e. whose couplings J correspond to the global minimum of $\mathcal{L}(m, J)$. Some of their findings, relevant to this work, are:

1. For any m_0 , the maximum value of $m_1(m_0)$ is obtained if $m = m_0$.
2. When $m \rightarrow 1^-$, the minimization of the $\mathcal{L}(m, J)$ trains a linear perceptron with N dimensional input/output layers (as in [11]) and maximal stability. This network will be referred to as a Support Vector Machine (SVM) [22].

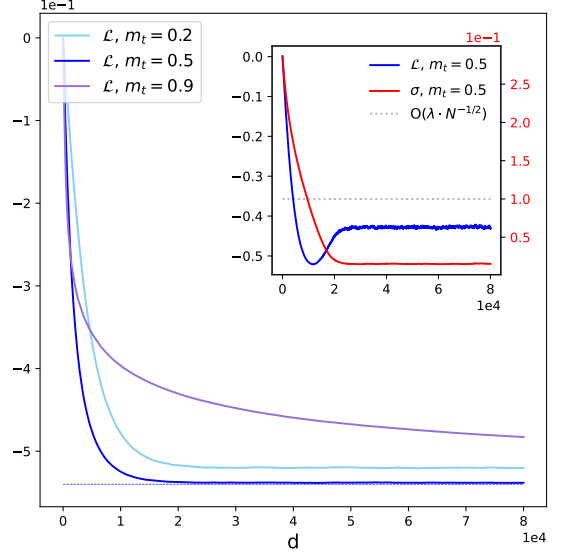


FIG. 3: The *blueish* lines in the main plot report the function $\mathcal{L}(m = 0.5, J)$ for different training overlaps as functions of the number of algorithm steps d . The *dotted* line represents the theoretical minimum value from [21]. The learning strength λ has been rescaled by the standard deviation of the couplings as described in the text. The subplot reports the case $m_t = 0.5$ when the learning strength is not rescaled: \mathcal{L} is in *blue*, while a measure of the standard deviation of the couplings, defined as $\sigma = \frac{1}{N} \sum \sigma_i$, is reported in *red*. The value $\lambda \cdot N^{-1/2}$ is also depicted in *light gray* to properly signal the moment when equation (16) loses its validity. All measures are averaged over 5 realizations of the couplings J . Choice of the parameters: $N = 100$, $\alpha = 0.3$, $\lambda = 1$, the initial couplings are Gaussian with unitary mean, zero variance and $J_{ii}^{(0)} = 0 \forall i$.

3. When $m \rightarrow 0^+$, the minimization of $\mathcal{L}(m, J)$ leads to a Hebbian coupling matrix $J_{ij} \propto J_{ij}^H$.

Numerically, we find that iterating 8 with a given value of m_t drives $\mathcal{L}(m_t, J)$ to its theoretical absolute minimum computed in [21], as reported in fig. 3 for one choice of N, α and m . This means that the performance of the training-with-noise algorithm can be completely described in the analytical framework of [21] and, in particular, all the above points hold. We are going to call $\mathcal{L}(m_t, J)$ loss function of the training-with-noise algorithm.

A. Classification

The computations contained in [21], and resumed in Appendix B, are now used to calculate n_{SAT} as a function

of m_t and α in the training-with-noise problem. The

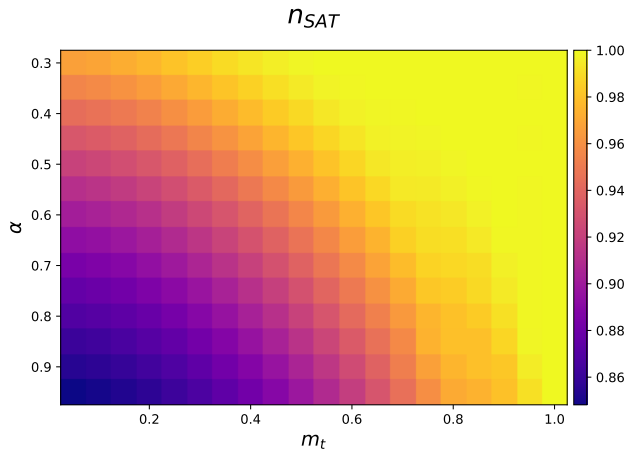


FIG. 4: n_{SAT} as a function of m_t and α . Warmer shades of colour are associated to higher classification performances.

distribution of the stabilities in the trained network (see equation B4) has always a tail in the negative values, except in the trivial case of $m_t = 1$, where $n_{SAT} = 1$ for $\alpha \leq 2$. This implies that classification is never reached by the training-with-noise algorithm. Nevertheless, the values of n_{SAT} remain close to unity for relatively high values of m_t and relatively low values of α (see fig. 4).

B. Generalization

The generalization properties of a network trained through training-with-noise are now discussed. The color map in fig. 5 reports the estimate of the retrieval map m_f at $m_0 = 1$ in the limit $N \rightarrow \infty$. Notice the emergence of two phases from the map: the *non retrieval* phase where $m_f(1)$ is mostly smaller than 0.5, and memories are far from being at the center of the basin; the *retrieval* phase where the $m_f(1)$ is higher, mostly close to 1, i.e. the memory is very close to the center of the basin. Such separation is typical of fully connected neural networks [3], differently from sparse neural networks [21, 23] where the topology of the basins results more various yet harder to get measured by experiments. In Appendix C we propose an empirical criterion to predict the transition between these two regimes. The resulting critical line is reported in fig. 5.

Fixing ourselves to the retrieval regime we employ a procedure described in Appendix C to compute the typical size of the basins of attraction of networks trained as

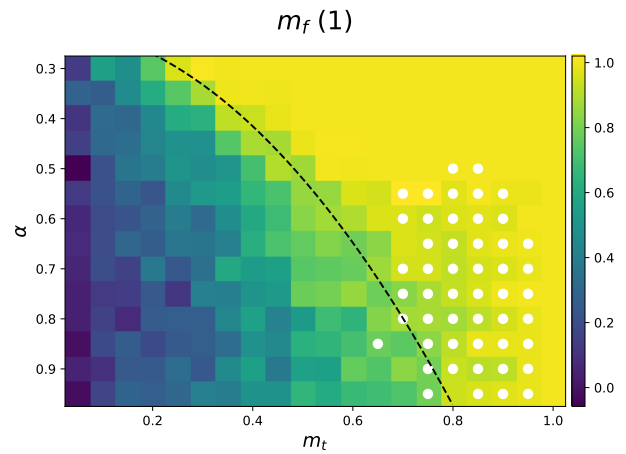


FIG. 5: $m_f(1)$ as a function of m_t and α . Warmer shades of colour are associated to higher retrieval performances. The *black dashed* line represents the boundary of the retrieval regime according to the criterion in Appendix C, *white* dots signal the points where basins of attraction to which memories belong are larger than ones obtained from a SVM at $N = 200$.

SVMs and with the training-with-noise algorithm. White dots in fig. 5 signal the combinations of (m_t, α) where the basins of attraction found by training-with-noise algorithm resulted smaller than the ones obtained by a SVM at the same value of α . We want to stress the importance of a comparison between the training-with-noise and the relative SVM, since numerical investigations have shown the latter to achieve very large basins of attraction, presumably due to the maximization of the stabilities [8, 17]. One can conclude that for most of the retrieval region the generalization performance is worse than the SVM, which maintains larger basins of attraction; on the other hand, at higher values of α the trained-with-noise network sacrifices its classification property to achieve a basin that appears wider than the SVM one. In conclusion, the training-with-noise algorithm never outperforms the relative SVM without reducing its classification capabilities.

V. TRAINING WITH STRUCTURED NOISE

In this section, we study how adding additional constraints on the configurations used in the training-with-noise algorithm affects its performance. This amounts to imposing specific internal dependencies among the noise units $\vec{\chi}$, which are no more i.i.d. random variables, as it was in [13]. When this choice is appropriate, the algorithm can lead to a classification regime and a high degree of generalization, resembling a SVM. We firstly evaluate the maximal noise case, i.e. $m_t = 0^+$ and derive a condition to be satisfied by noisy data-points to approach the best memory performance. In light of such

condition, we analyze the performance of fixed points of the dynamics as training data. Finally, we run training-with-noise with $m_t > 0$ using fixed points of the dynamics as training-data, after initializing the coupling according to Hebb's rule. We find that the structure of noise is relevant also in this case. It will be helpful for our purposes to implement a symmetric version of rule (8), i.e.

$$\delta J_{ij}^{(d)} = \frac{\lambda}{N} (\epsilon_i^{\mu_d} \xi_i^{\mu_d} S_j^{\mu_d} + \epsilon_j^{\mu_d} \xi_j^{\mu_d} S_i^{\mu_d}) \quad (17)$$

Equation (17) can be rewritten explicitly making use of (9), leading to

$$\begin{aligned} \delta J_{ij}^{(d)} = & \frac{\lambda}{2N} (\xi_i^{\mu_d} S_j^{\mu_d} + S_i^{\mu_d} \xi_j^{\mu_d}) + \\ & - \frac{\lambda}{2N} (S_i^{1,\mu_d} S_j^{\mu_d} + S_i^{\mu_d} S_j^{1,\mu_d}) \end{aligned} \quad (18)$$

where $S_i^{1,\mu_d} = \text{sign} \left(\sum_{k=1}^N J_{ik} S_k^{\mu_d} \right)$. The total update to the coupling at time D can be decomposed as a sum of two contributions

$$\Delta J_{ij}(D) = \Delta J_{ij}^N(D) + \Delta J_{ij}^U(D). \quad (19)$$

The first term on right-hand side, which will be referred to as *noise* contribution, is expressed in terms of noise units as

$$\Delta J_{ij}^N(D) = \frac{\lambda}{2N} \sum_{d=1}^D \xi_i^{\mu_d} \xi_j^{\mu_d} \chi_j^{\mu_d} + \frac{\lambda}{2N} \sum_{d=1}^D \xi_j^{\mu_d} \xi_i^{\mu_d} \chi_i^{\mu_d}, \quad (20)$$

while the second term, which will be referred to as *unlearning* contribution, is given by

$$\Delta J_{ij}^U(D) = -\frac{\lambda}{2N} \sum_{d=1}^D (S_i^{1,\mu_d} S_j^{\mu_d} + S_i^{\mu_d} S_j^{1,\mu_d}). \quad (21)$$

A. $m_t = 0^+$

Training configurations with maximal noise are now studied. Firstly, we apply eq. (19) to compute the variation of $\mathcal{L}(m, J)$ during training, showing what are the properties of the training configurations that lead to a good network performance. Then we numerically probe two types of attractor landscapes to study the distribution of the good training data. Eventually, we consider fixed points of the dynamics (1) as training configurations, showing a connection between the training-with-noise and unlearning algorithms.

The optimal structure of noise

We now want to study what kind of noise structure is favorable to achieving classification and a good degree of

generalization. Section (IV) has shown that the training-with-noise algorithm on fully connected networks never outperforms a SVM without reducing their classification properties. In addition to this, we know from numerics [8, 17] that SVMs, as maximally stable perceptrons, maximize the size of the basins of attraction of the memories as they are also attractors of the dynamics. We hence consider the SVMs as optimal recurrent networks in both terms of classification and generalization. As a consequence, we just need to approach the global minimum of $\mathcal{L}(m = 1^-, J)$ to train a well performing neural network. During the rest of this work we will apply an important differentiation between the two variables m and m_t : while the former controls the final result of the optimization procedure, the latter is a fixed level of noise, $m_t = 0^+$ in the current case. According to the training-with-noise algorithm, at $m_t = 0^+$ the variation of $\mathcal{L}(m, J)$ is $\delta \mathcal{L} = \delta \mathcal{L}_N + \delta \mathcal{L}_U$, where $\delta \mathcal{L}_N$ cancels in time, and the only relevant contribution is

$$\delta \mathcal{L}_U \propto \frac{m}{\sqrt{2(1-m^2)}} \sum_{i,\mu}^{N,p} \omega_i^\mu \exp \left(-\frac{m^2 \Delta_i^{\mu^2}}{2(1-m^2)} \right), \quad (22)$$

where

$$\omega_i^\mu = \frac{1}{2\sigma_i} \left(m_\mu \chi_i^{1,\mu} + m_{1,\mu} \chi_i^\mu \right), \quad (23)$$

with

$$\chi_i^\mu = \xi_i^\mu S_i^{\mu_d} \quad \chi_i^{1,\mu} = \xi_i^\mu S_i^{1,\mu_d}, \quad (24)$$

and

$$m_\mu = \frac{1}{N} \sum_{j=1}^N S_j^{\mu_d} \xi_j^\mu \quad m_{1,\mu} = \frac{1}{N} \sum_{j=1}^N S_j^{1,\mu_d} \xi_j^\mu. \quad (25)$$

The derivation of (22) is reported in Appendix A 2. For the case of fixed points, we have $\omega_i^\mu = m_\mu \chi_i^\mu$, coherently with the same observable defined in [8]. Generally speaking, ω_i^μ can be a function of Δ_i^μ . Since stabilities are self-averaging quantities, by taking $N, p \gg 1$ we can rewrite equation (22) as

$$\delta \mathcal{L}_U \propto \frac{m}{\sqrt{2\pi(1-m^2)}} \int_{-\infty}^{+\infty} d\Delta \rho(\Delta) \omega(\Delta) e^{-\frac{m^2 \Delta^2}{2(1-m^2)}}, \quad (26)$$

where $\rho(\Delta)$ is the true probability density function of Δ at a given step of the algorithm. When $m \rightarrow 1^-$ the Gaussian contained in the integral becomes very peaked around 0. Since ρ is a strictly positive function, and we want $\delta \mathcal{L}$ to decrease, we need

$$\omega(\Delta) < 0 \quad \text{when} \quad |\Delta| < \epsilon, \quad \epsilon = 0^+ \quad (27)$$

Hence, a coupling update improves the memory performances when condition (27) is satisfied. As a consequence, noisy units are internally constrained by (27), as a difference with the standard training-with-noise algorithm. The more negative ω is when $\Delta \sim 0$ the more powerful a given data-point is at approaching the SVM performances. One should also bear in mind that training is a dynamic process: to reduce $\mathcal{L}(m = 1^-, J)$ condition (27) should hold during training.

About the initialization

We are now interested in studying how the initialization of the couplings influences the choice of training configurations, concentrating in particular on the function $\omega(\Delta)$. Computing ω analytically is a challenging task, but we will introduce some related empirical quantities, which can be useful to probe the structure of noise in the configurations. To do so, we first sample training configurations from a network initialized with the Hebbian rule according to a Monte Carlo dynamics at temperature T . Temperature acts as a control parameter: when $T = 0$ training configurations are stable fixed points of eq. (1), as in standard unlearning. Higher values of T progressively reduce the structure of noise in training configurations, and in the limit $T \rightarrow \infty$, training configurations are the same as in the training-with-noise algorithm. The Monte Carlo of our choice is of the Kawasaki kind [24], to ensure that all training configurations are at the prescribed overlap $m_t = 0^+$. Fig. 6, presents the result at four different temperatures. Each panel shows ω as a function of Δ . Data points are collected over 15 realizations of the network, then plotted and smoothed to create a density map. We are interested in the *typical* behavior of $\omega(\Delta)$ in the neighborhood of $\Delta = 0$, which can be estimated by a linear fit of the data. We consider the intercept of the best fit line as an *indicator* $\omega_{emp}(0)$ of the mean value of $\omega(0)$ over the noise.

We find that the lower the temperature, the more sampled configurations favor both classification and generalization: the line is negative over a larger interval centered around $\Delta = 0$. As temperature becomes too high, $\omega_{emp}(0)$ gets closer to zero, suggesting low quality in terms of training performance.

Another interesting aspect emerged from the analysis is that, by calling a the line intercept and b its angular coefficient, the position of the right extremum of the negative band $\frac{|a|}{b}$ is independent of the system size N , implying that finite size effects are not strong for this kind of measure. This is likely because both the mean of the distribution of the points along ω and their dispersion, i.e. how far they span the y-axis, are decreasing as $O(N^{-1/2})$.

The same analysis is repeated in the case of a random initialization. We chose the Sherrington-Kirkpatrick (SK) model [25] as a case of study. Panels (a) and (b) in fig. 7 report the smoothed distribution of ω versus Δ showing a different scenario with respect to the Hebbian one. The distribution looks anisotropic, as in the Hebbian case, yet the stabilities are centered Gaussians, so $\omega_{emp}(0)$ is positive. In particular, things appear to improve when T increases, in contrast with the previous case of study, though in accordance with the Hebbian limit of the training-with-noise algorithm explained in Section IV. Panel (c) displays more clearly the mutual dependence between ω and stabilities Δ by reporting the Pearson coefficient at the various T between these two quantities: both Hebb's and SK show some mutual dependence, but the distribution in the Hebbian landscape

is way more deformed. Furthermore, panel (d) shows $\omega_{emp}(0)$ in both cases. This quantity is very well correlated with the Pearson coefficient: whereas in the Hebb's initialization $\omega_{emp}(0)$ remains negative and reaches the lowest values at low temperatures, the random case shows an opposite trend, where the estimated $\omega_{emp}(0)$ is rather positive. Notice, from both panels (c), (d), the existence of an optimum which does not coincide with the stable fixed points of the dynamics (i.e. $T = 0$): this aspect will be deepened in Sec. VI.

Training with stable fixed points

Let us now consider the instance of a set of noisy states that are also fixed points of the dynamics with a training overlap $m_t = 0^+$. In this case, one has

$$\Delta J_{ij}^N(D) = 0^+ + O\left(\sqrt{\frac{\lambda}{N}}\right). \quad (28)$$

On the other hand, the unlearning contribution to the evolution of the couplings is

$$\Delta J_{ij}^U(D) = -\frac{\lambda}{N} \sum_{d=1}^T S_i^{\mu_d} S_j^{\mu_d}, \quad (29)$$

which is the classic unlearning updating rule. As a result, when $\lambda/N \rightarrow 0$ the training-with-noise algorithm and the unlearning algorithm will converge to the same updating rule for the couplings when stable fixed points of the dynamics are used in the training. The same argument can be applied to the original asymmetric rule (8), however asymmetric networks may have no stable fixed points of (1) that can be learned.

We now perform a numerical test of the argument above, in the case of a symmetric connectivity matrix. At each step of the algorithm, the network is initialized with an initial overlap contained in $(0, N^{-1/2})$ with one memory ξ^{μ_d} . Then, asynchronous dynamics (1) is run until convergence, and the final overlap m_t is measured. If $m_t \in (0, N^{-1/2})$, we use the sampled configuration for training, otherwise the process is repeated. Typically, an initial overlap equal to 0^+ implies a similar order of magnitude for the final overlap, hence no reiteration is needed.

The algorithm (17) is repeated for $D^* = O(N/\lambda)$ steps. The order of magnitude of $\Delta J_{ij}^U(D)$ is supposed to be the same of $J_{ij}^{(0)}$, in order to see significant modifications to the initial connectivity matrix. The network is initialized according to the Hebb's rule (2), i.e. $J_{ij}^{(0)} = O(N^{-1/2})$ which implies $\Delta J_{ij}^U(D) = O(N^{-1/2})$ at leading order. The contributions U and N are compared by computing the norm of the relative ΔJ matrix and evaluating the ratio $|\Delta J^U|/|\Delta J^N|$. From our previous considerations we expect $|\Delta J^U|/|\Delta J^N|$ to be linear in $\lambda^{-1/2}$ when corrections vanish. Results are reported in fig. 8:

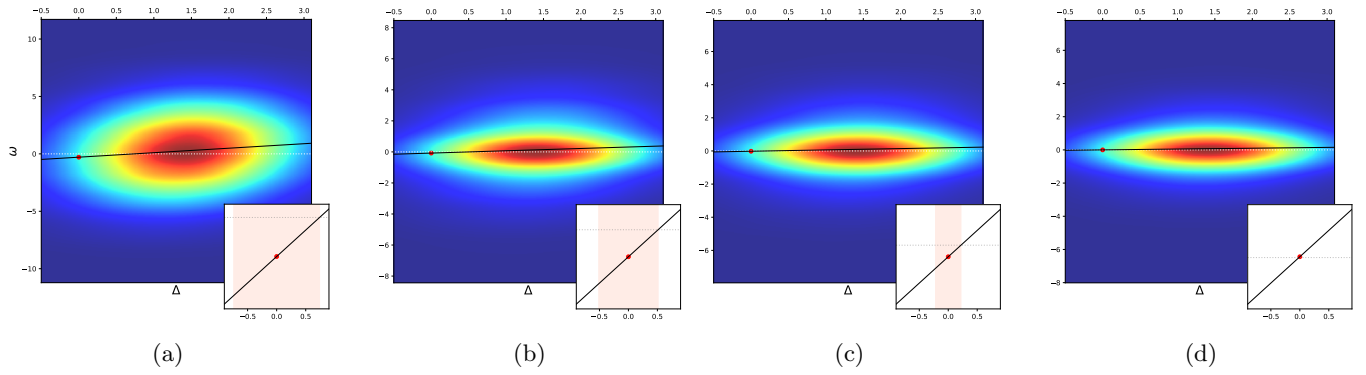


FIG. 6: Distribution of ω_i^μ as a function of Δ_i^μ for training configurations sampled with a Monte Carlo at temperature $T = 0$ i.e. stable fixed points only (a), $T = 0.5$ (b), $T = 1$ (c), $T = 8$ (d), on a Hebbian network. Warmer colors represent denser region of data points. The *full black* line is the non-weighted best fit line for the points, the *dotted white* line represents $\omega = 0$, the *red dot* is the value of the best fit line associated with $\Delta = 0$. Sub-panels to each panel report a zoom of the line around $\Delta = 0$: the *reddish* region give a measure of the largeness of the negative band centered around $\Delta = 0$. Measures have been collected over 15 samples of the network. Choice of the parameters: $N = 500$, $\alpha = 0.5$.

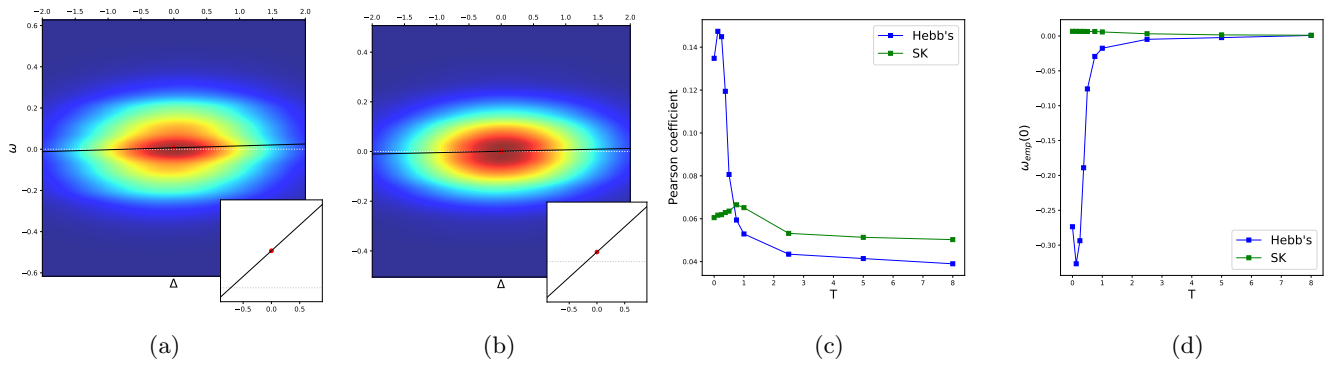


FIG. 7: (a), (b): Distribution of ω_i^μ as a function of Δ_i^μ for training configurations sampled with a Monte Carlo at temperature $T = 0$ i.e. stable fixed points only (a), and $T = 8$ (b) on a SK model. Warmer colors represent denser region of data points. The *full black* line is the non-weighted best fit line for the points, the *dotted white* line represents $\omega = 0$, the *red spot* is the value of the best fit line associated with $\Delta = 0$. Sub-panels to each panel report a zoom of the line around $\Delta = 0$. (c), (d): Comparison between the Hebbian initialization and the Random one through evaluation of: the Pearson coefficient between ω_i^μ and Δ_i^μ (c) and the estimated value of $\omega_{emp}(0)$ from the dispersion plots (d). Measures have been collected over 15 samples of the network. Choice of the parameters: $N = 500$, $\alpha = 0.5$.

$|\Delta J^U|/|\Delta J^N|$ grows when N increases and λ decreases, according to the scaling relation predicted by our argument. In addition to this, curves are collapsing on the expected line when $\lambda \rightarrow 0$ and $N \rightarrow \infty$.

We also measured Δ_{min} at its maximum over the course of the algorithm (as described in IV A). Results are reported in fig. 9. Δ_{min} produced by training-with-noise and unlearning are found to coincide when λ is sufficiently low. Moreover, the number of steps necessary to reach the maximum are the same for both the algorithms, confirming that couplings are transforming in the same way. This last aspect is corroborated by the

subplot in fig. 9, representing the set of J_{ij} obtained with the traditional unlearning algorithm as a function of the one resulting from the training-with-noise algorithm, for one realization of the network. The strong correlation is evident, as predicted from our pseudo-analytical arguments.

One can also study how $\omega(\Delta)$ evolves during the training process. Fig. 10a shows the value of $\omega_{emp}(0)$ at different time steps of the training process, for different values of α . The colored halo around the line of data points represents the width of the band centered in 0 where the line of the best fit assumes negative values.

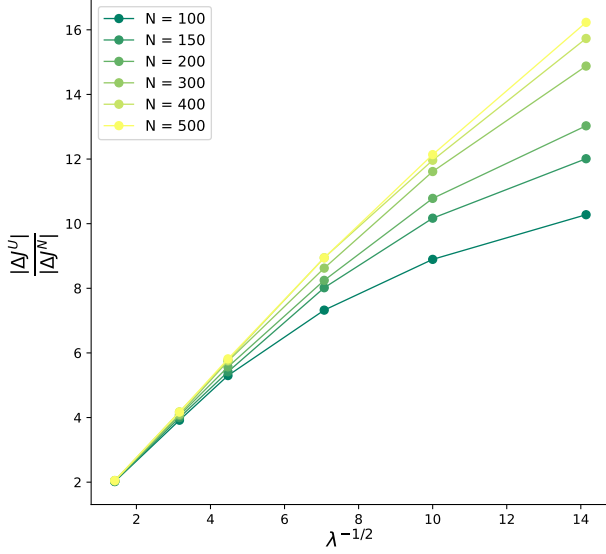


FIG. 8: Estimates of the ratio $|\Delta J^U|/|\Delta J^N|$ as a function of $\lambda^{-1/2}$ and N for $\alpha = 0.5$. Measures are averaged over 5 samples. Error bars are not indicated because smaller than the symbols.

We find that $\omega_{emp}(0) < 0$ for $\alpha \leq 0.6$. The progressive increase of $\omega_{emp}(0)$ means that the structure of the fixed points is more effective in the starting Hebbian landscape compared to intermediate stages of training. In the last part of training, points reacquire more negative values, but this is not a reliable indication of good performance: as shown in fig. 10c, in this part of the process the standard deviation of the couplings σ_i is comparable to $O(\lambda \cdot N^{-1/2})$, and the expansion of the \mathcal{L} in eq. (22) is not valid. The last part of the training, where $\sigma_i \simeq 0 \forall i$, has been neglected from the plot. On the other hand, the width of the colored halos decreases with α . The experiment is thus consistent with the characterization of the unlearning algorithm presented in [8], which showed decreasing classification and generalization when increasing α . This is confirmed by the study of the Pearson correlation coefficient between ω_i^μ and the associated stabilities Δ_i^μ (see Fig. 10,b). High values of the Pearson coefficient show a strong dependence of the structure of noise on the relative stabilities. For all α , the Pearson coefficient is highest at $d = 0$, and progressively decreases during training, suggesting that the quality of the training configurations is deteriorating. The final increase in the coefficient is, again, due to the vanishing of the standard deviations σ_i of the couplings, and does not indicate good performance.

B. $m_t > 0$

When training configurations are fixed points of the dynamics with $m_t = O(1)$, the considerations of the pre-

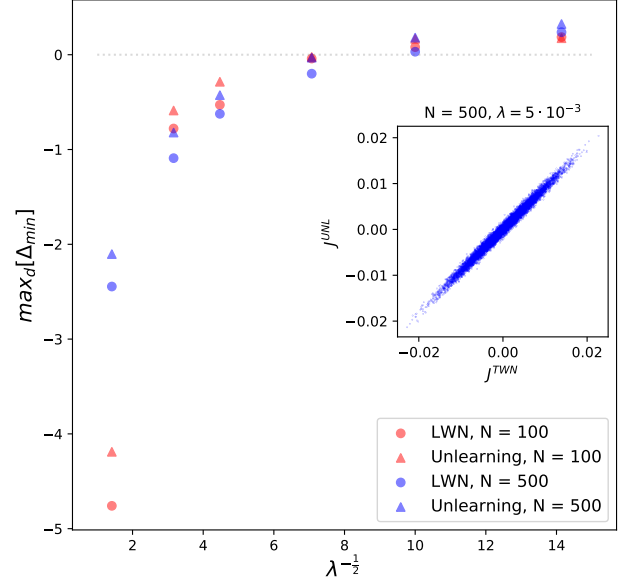


FIG. 9: The quantity $\max_d(\Delta_{\min})$ as a function of $\lambda^{-1/2}$. Colors are: *red* for $N = 100$ and *blue* for $N = 500$. The *gray* line represents the null value for the stability. Symbols are: *circles* for the training-with-noise rule, *triangles* for the unlearning rule. In the subplot on the center right, the couplings obtained through the unlearning algorithm are plotted as a function of the ones resulting from the training-with-noise, at the same amount of iterations, for one sample at $N = 500$ and $\lambda = 5 \cdot 10^{-3}$. Measures are averaged over 50 samples. The choice of the parameters is: $\alpha = 0.5$, $m_t = 0^+$.

vious section no longer apply. Such configurations can be generated by initializing the network at an overlap $m = O(1)$ with a memory, and let it evolve according to (1). The connectivity matrix is initialized according to Hebb's learning rule eq. (2). In this setting, if at some point during training m happens to enter the basin of attraction of the memories, the fixed point reached by the dynamics will be the memory itself, and the noise contribution will cancel exactly the learning contribution, giving $\delta J = 0$. On the other hand, for sufficiently high values of the load α , at the start of the training procedure memories will have zero size basins of attraction and trajectories will drift away from the memories following the dynamics. In this scenario, the two contributions δJ^N and δJ^U decorrelate, and δJ^N will take again a similar role to what described in the previous section. The result is an algorithm which interpolates between unlearning when d is small and a supervised algorithm when basins increase to a size close to $(1 - m)$. In this regime, δJ^N acts as a breaking term, preventing the algorithm to further modify the coupling matrix J . A similar mechanism has been studied in [26] where a supervised term was added to the standard unlearning update rule, leading to $\delta J_{ij} \propto -S_i^{\mu_d} S_j^{\mu_d} + \xi_i^{\mu_d} \xi_j^{\mu_d}$. Notice that the term

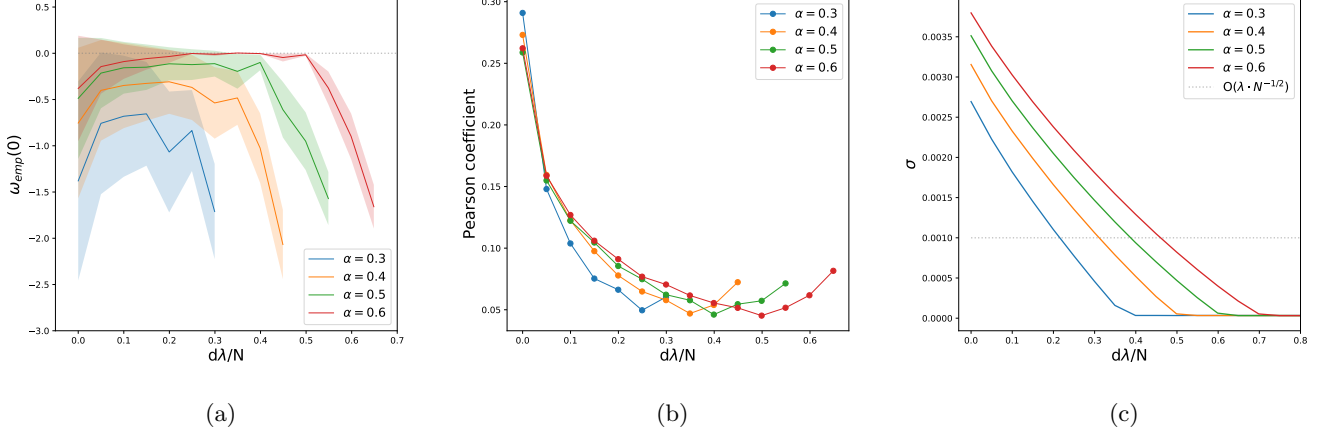


FIG. 10: The training-with-noise algorithm is implemented by sampling stable fixed points of the network dynamics with $m_t = 0^+$. (a) The empirical measure of ω for $\Delta = 0$ for the stable fixed points as a function of the rescaled number of iterations of the training-with-structured-noise algorithm: the bars represent the symmetric negative band obtained from the linear fit in fig. 6. (b) Pearson coefficient measured between ω_i^μ and Δ_i^μ . (c) The standard deviation of the couplings during learning, defined as $\sigma = \frac{1}{N} \sum \sigma_i$. Points are averaged over 50 samples and the choice of the parameters is: $N = 100$, $\lambda = 10^{-2}$.

$\xi_i^{\mu d} \xi_j^{\mu d}$ is deterministically reproducing Hebb's learning rule, while in our study the unlearning is modified by a stochastic term, whose nature we have already discussed. Given a sufficiently small learning rate λ , there will exist a characteristic number of steps of the algorithm over which the coupling matrix does not change significantly. We will call this timescale *an epoch*. Averaging the effect of training steps over an epoch, we get a snapshot of how the algorithm is affecting the couplings at a given point during training. This can be used to study the relation between δJ^N and δJ^U , quantified by the connected correlation coefficient

$$\text{Cov}_{N-U} := \frac{2}{N(N-1)} \sum_{i,j>i} (\overline{\delta J_{ij}^N \delta J_{ij}^U} - \overline{\delta J_{ij}^N} \overline{\delta J_{ij}^U}), \quad (30)$$

where the average is computed over an epoch. When this quantity equals one, there is no effective update of the couplings over an epoch. Results are presented in fig. 11 for different values of m and of α , as a function of the number of training steps d . The number of iterations has been rescaled by a factor p/λ for clarity of the plot. At any given α , training with higher m results in a faster increase of Cov_{N-U} , i.e. a faster convergence of the algorithm. If the value of m is too low, the algorithm never manages to build a big enough basin of attraction, and never stops. As α is increases, higher and higher values of m are required for the algorithm to stop, since the typical size of the attraction basins shrinks.

The network performance can be benchmarked by tracking the evolution of the lowest stability Δ_{\min} throughout the training procedure. Results are presented in fig. 12 for different values of α and m . For sufficiently low values of α and sufficiently high values of m , Δ_{\min}

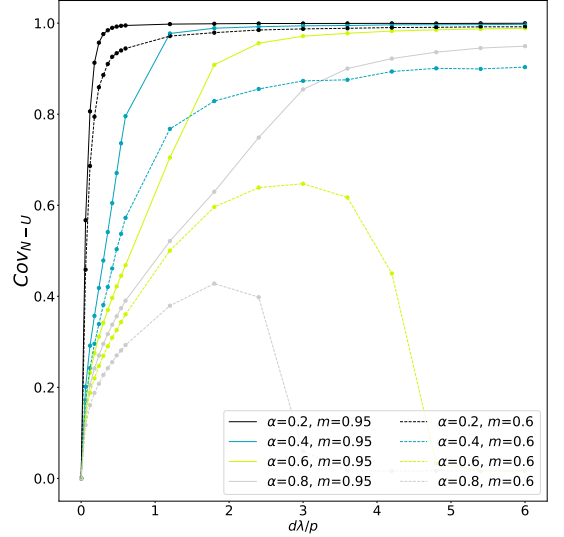


FIG. 11: Correlation between *noise* and *unlearning* contributions to δJ as a function of the rescaled number of training steps $\frac{d\lambda}{p}$, for two values of the training parameter m , and different values of α . When $\text{Cov}_{N-U} = 1$, the algorithm stops modifying the coupling matrix. Choice of the parameters: $N = 400$, $\lambda = 10^{-2}$. Results are averaged over 100 samples.

surpasses the zero. Once this condition is met, the value Δ_{\min} becomes essentially constant, even if $\text{Cov}_{N-U} < 1$, signaling that the update of the coupling matrix is still in progress. The result is a curve $\Delta_{\min}(d)$ which barely surpasses zero. For each value of m there exists a critical

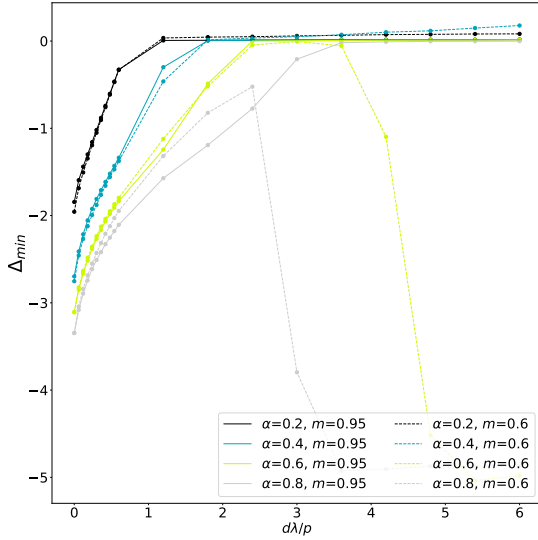


FIG. 12: Minimum stability as a function of the rescaled number of training steps $\frac{d\lambda}{p}$, for two values of the training parameter m , and different values of α . When $\Delta_{\min} \geq 0$, each memory is a stable fixed point of the dynamics. Choice of the parameters: $N = 400$, $\lambda = 10^{-2}$. Results are averaged over 100 samples.

value $\alpha_c(m)$ beyond which no amount of steps is able to produce $\Delta_{\min} > 0$. Extrapolating empirical results to the $N \rightarrow \infty$ limit, one finds

$$\alpha_c(m) = A \cdot (m)^B + C,$$

where

$$A = 0.35 \pm 0.01, \quad B = 6.9 \pm 0.5, \quad C = 0.58 \pm 0.01$$

Consistently with what presented in the previous section, in the limit $m \rightarrow 0^+$ one finds the critical capacity of the unlearning algorithm [6, 8]. The critical capacity increases up to a value $\alpha_c(1) = 0.93 \pm 0.01$ when m reaches unity.

Regardless of whether $\Delta_{\min} > 0$ is obeyed, one can monitor the network performance as an associative memory device by measuring the retrieval map $m_f(m_0)$. We find that the best performance always corresponds to the number of training step maximizing Δ_{\min} , hence the curves $m_f(m_0)$ are all relative to this number of steps. Results are presented in fig. 13. When classification is achieved (i.e. $\alpha < \alpha_c(m)$), lower values of m increase the degree of generalization of the network (i.e. enlarge the basins of attraction), at the cost of a lower critical capacity.

VI. A SAMPLING PROCEDURE FOR NOISY DATA-POINTS

Insights from the previous sections on the structure of well performing training data can be used to effectively

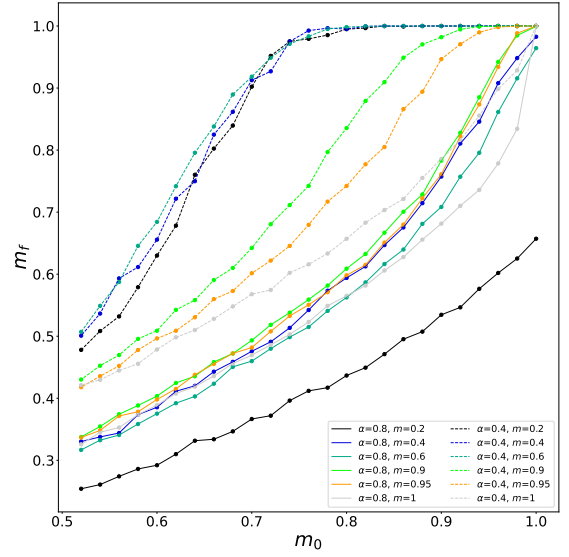


FIG. 13: Retrieval map $m_f(m_0)$ for two values of α and different values of the training parameter m . At $\alpha = 0.4$, every m leads to stable memories, i.e. $m_f(1) = 1$. At $\alpha = 0.8$, only the highest values of m lead to stable memories, while for low values of m one has $m_f(1) < 1$. Choice of the parameters: $N = 400$, $\lambda = 10^{-2}$. Results are averaged over 100 samples.

sample configurations to teach to the model. This can be achieved by means of a supervised Monte Carlo routine that searches for maximally noisy configurations (i.e. $m_t = 0^+$) satisfying condition (27). The coupling matrix is initialized according to Hebb's rule (2), and updated recursively according to either eq. (8) or eq. (5). We first introduce the sampling algorithm and then report some numerical results regarding both the training-with-noise and unlearning routines.

A. The sampling algorithm

We sample maximally noisy training configurations $m_t = 0^+$ such that $E(\vec{\chi}|m, J) < 0$, where

$$E(\vec{\chi}|m, J) := \frac{m}{\sqrt{2(1-m^2)}} \sum_{i,\mu} \omega_i^\mu \exp\left(-\frac{m^2 \Delta_i^{\mu^2}}{2(1-m^2)}\right), \quad (31)$$

that is a function of the noisy variables χ_i^μ , conditioned on a reference overlap m and the couplings J . Sampling is done through the following procedure:

1. The network is initialized in a random configuration and the asynchronous dynamics in eq. (1) is run until convergence on a fixed point. The final state \tilde{S}^{μ_d} must have an overlap m_t in the interval $(0, 1/\sqrt{N})$ with one memory μ_d , otherwise the procedure is repeated.
2. A $T = 0$ temperature dynamics in the landscape of $E(\vec{\chi}|m, J)$ is performed until $E(\vec{\chi}|m, J) < 0$. We

use a Kawasaki kind of dynamics over the noisy variables $\vec{\chi}$ to make sure that m_t maintains the prescribed value.

Since $E(\vec{\chi}|m, J)$ is proportional to $\delta\mathcal{L}_U$ (see eq. (22)), the procedure will lead to a reduction in the Loss eq. (14). In this setting, the classification and generalization properties can be tuned by the parameter m , while the training configurations always have a fixed value of $m_t = 0^+$. In particular, to require a performance that is most similar to the one of a SVM, we will set $m \rightarrow 1^-$.

The sampling procedure starts from fixed points because we know, from the previous sections, that they are close to be the most effective configurations. Interestingly, the described procedure results significantly more effective than a standard minimization of $\mathcal{L}(m = 1^-, J)$: in the latter case training stops when $\mathcal{L} = -1$, while the former technique apparently pushes the stabilities further in the positive values. Nevertheless, the goal of this section is not to propose a winning, or more computationally efficient training routine, but rather to search for the most virtuous training data points in the context of maximal training noise, and reveal their identity.

B. Algorithm performance

The sampling procedure results in a better performance for both training-with-noise and the unlearning update rules. Results for training-with-noise are reported in fig. 14. Panel (a) shows that classification is reached up to $\alpha \simeq 0.8$ for a network of size $N = 100$. Panel (b) shows the retrieval map $m_f(m_0)$, for different values of α and for the lowest number of algorithm iterations leading to classification. The high values of m_f for $m_0 \sim 1$ indicates that the network, while achieving classification, maintains good generalization properties. Results for a SVM with the same control parameters are also shown, for comparison. The curves obtained from the training-with-noise are higher than ones relative to the SVM, signaling a better recalling performance, even though quantifying this effect will require a more detailed study of finite size effects. Fig. 15 shows analogous plots for the unlearning update rule. Again, the network compares favorably with traditional unlearning in terms of memory capacity, that is increased up to $\alpha \simeq 0.9$ (see panel (a)) with respect to the maximum capacity of $\alpha \simeq 0.7$ obtained with fixed points only. Panel (b) represents an indication for the sizes of the basins of attraction at the lowest number of algorithm iterations leading to classification. Results are coherent with fig. 1 concerning $\alpha = 0.35$, yet again basins appear to be larger than the ones from a SVM trained with the same control parameters.

The role of saddles

Virtuous training configurations picked by the sampling algorithm are generally not fixed points of the dynamics eq. (1). To conclude the study, we characterized them in terms of their *saddle index* f , namely the ratio between the number of unstable sites under the dynamics (see eq. (1)) and the total number of directions N . Stable fixed points have $f = 0$, while random configurations are expected to have $f = 1/2$. Panel (c) in fig. 14 and fig. 15 report the behavior of the saddle index f of the sampled configurations as a function of the number of steps of the algorithm, relatively to training-with-noise and unlearning respectively. Most of the sampled training configurations are low index saddles. This observation is consistent with the results in Section V A relative to the landscape of attractors for the Hebb's rule, where we associate low saddles to the configurations probed by a Monte Carlo at low temperatures. This is also supported by previous studies on spin glasses [27].

In order to check whether f is indeed capturing relevant features of the virtuous training configurations, we have repeated the training procedure, sampling training data according to the sole requirement that their saddle fraction be a specific value f . This is done by randomly initializing the network on a configuration having training overlap $m_t = 0^+$ with a reference memory, and performing a $T = 0$ temperature dynamics on the landscape defined by the energy

$$E(\vec{S}|f, J) = \frac{1}{2} \left(\frac{1}{N} \sum_{i=1}^N \Theta(S_i \sum_{j=1}^N J_{ij} S_j) - f \right)^2, \quad (32)$$

where $\Theta(x)$ is the Heaviside function. Yet again, the value of m_t was maintained constant during the descent. Fig. 16 shows how the minimum stability evolves during the training process while a symmetric training-with-noise algorithm is initialized in the Hebbian matrix and learns saddles of different indices. For a network of $N = 100$ and $\alpha = 0.35$, we found that classification is reached until quite high values of f , suggesting that such saddles are indeed good training data. Notice, in particular, that the range of saddles indexes that support good training performances are consistent with the ones spanned by the points in the sub-panel in fig. 14c. It should be stressed that the precise performance as a function of f is quite sensitive to the sampling procedure. Simulated annealing routines [28] have been also employed to minimize (32), obtaining qualitatively similar results yet not coinciding with the ones reported in fig. 16. A qualitative study of the basins of attraction of the network has been performed and reported in a sub-plot in fig. 16. In particular, the retrieval map $m_f(m_0)$ has been measured relatively to the saddle indices f at the first time they reached classification, in analogy to what has been measured in [8]. The curves coincide quite well, suggesting that finite sized networks trained with

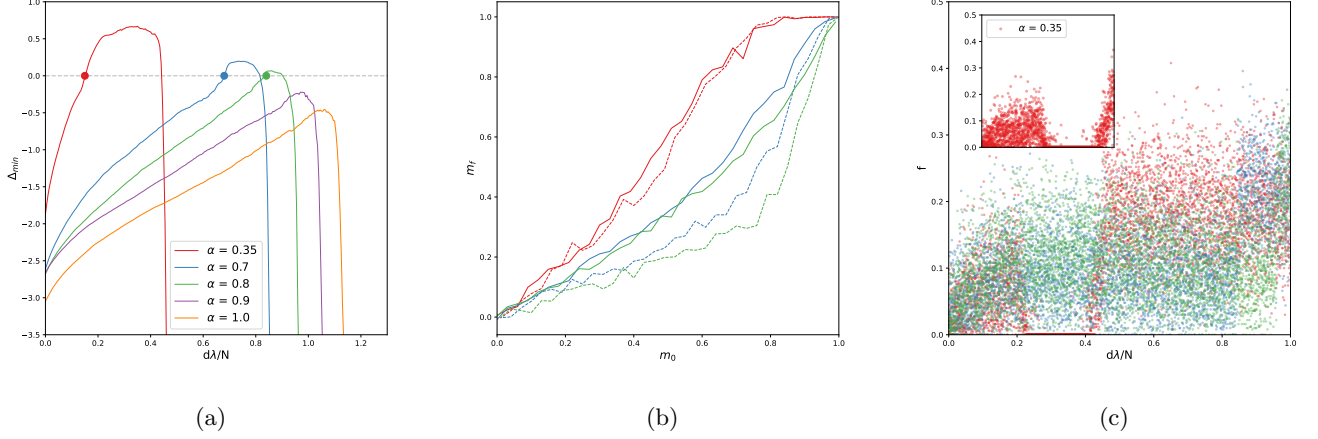


FIG. 14: Performance of the training-with-noise algorithm taught with noisy configurations sampled according to Section VI regarding four progressing values of the load α . (a) Minimum stability as a function of the algorithm time: *full* line is the unlearning with sampling, *dotted* line is the traditional unlearning. (b) Retrieval map $m_f(m_0)$, relatively to the *circles* in panel (a) for $\alpha \in [0.35, 0.7, 0.8]$: *full* line is the unlearning with sampling, *dashed* line is a SVM trained with no symmetry constraints with the same control parameters. (c) Saddle index f as a function of the algorithm steps for $\alpha \in [0.35, 0.7, 0.8]$. The sub-panel zooms over $\alpha = 0.35$ alone. All data points have been averaged over 20 samples in (a),(b) and 5 samples in (c). Errors are neglected for clarity of the image. The choice of the parameters: $N = 100$, $\lambda = 10^{-3}$, $m = 0.9999$.

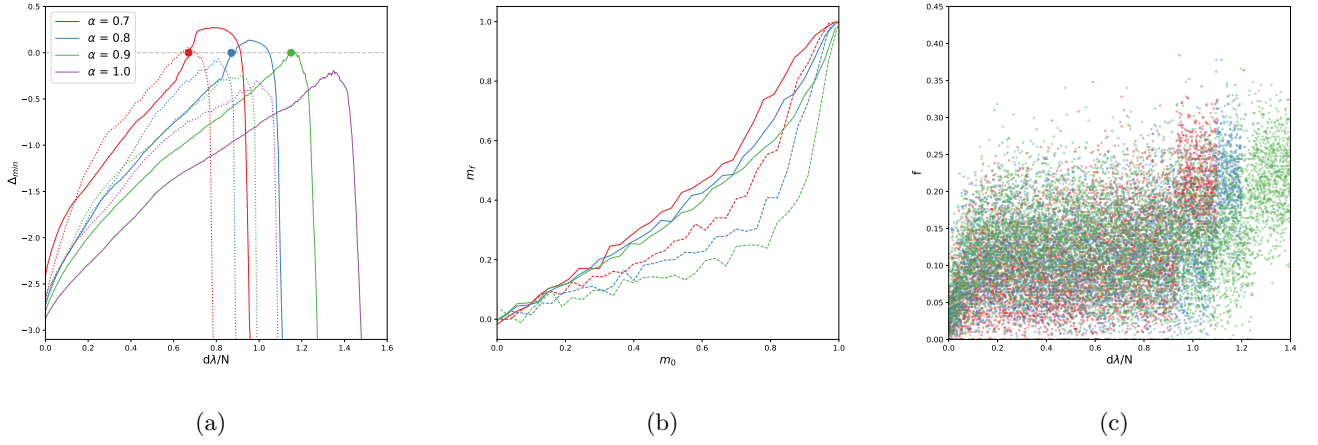


FIG. 15: Performance of the unlearning algorithm trained with noisy configurations sampled according to Section VI regarding four progressing values of the load α . (a) Minimum stability as a function of the algorithm time: *full* line is the unlearning with sampling, *dotted* line is the traditional unlearning. (b) Retrieval overlap $m_f(m_0)$, relatively to the *circles* in panel (a) for $\alpha \in [0.7, 0.8, 0.9]$: *full* line is the unlearning with sampling, *dashed* line is a SVM trained with no symmetry constraints with the same control parameters. (c) Saddle index f as a function of the algorithm steps for $\alpha \in [0.7, 0.8, 0.9]$. All data points have been averaged over 20 samples in (a),(b) and 5 samples in (c). Errors are neglected for clarity of the image. The choice of the parameters: $N = 100$, $\lambda = 10^{-3}$, $m = 0.9999$.

different f assume similar volumes of the basins of attraction when they are measured at the very first instant they reach classification. The plot also shows that the generalization performance is comparable with the one of a SVM trained with the same choice of the control parameters, consistently with the results of [8] in the matter

of the unlearning algorithm.

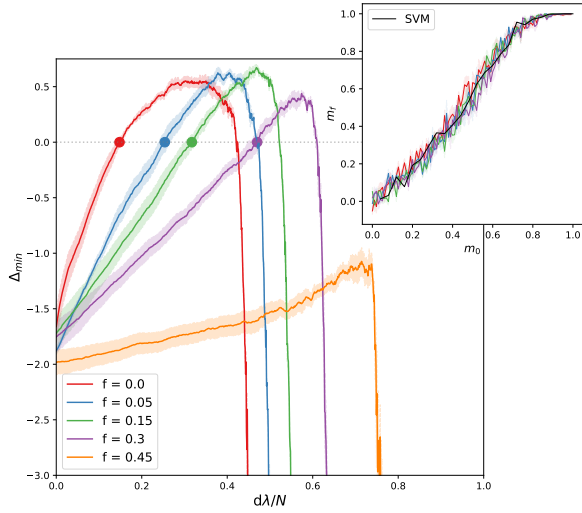


FIG. 16: Minimum stability Δ_{\min} as a function of the algorithm steps on a network trained with the symmetric training-with-noise routine that learns saddles of various indices f . The initial matrix is assembled according to the Hebb's rule. Full dots report the amount of iterations needed to accomplish classification. The subplot depicts the relation $m_f(m_0)$ as measured on the positions of the dots. A comparison with a SVM trained with the same choice of the parameters is presented. All measures are averaged over 5 samples with the shaded region indicating the experimental errors. The choice of the parameters is: $N = 100$, $\alpha = 0.35$, $\lambda = 10^{-3}$.

VII. CONCLUSIONS

The seminal work of [13] showed that noise could be injected during training to increase generalization, i.e. the capability of neural networks to retrieve classes of data by receiving corrupted stimuli [29–32]. The same concept recently seems to catch on in biology as well [33, 34], as artificial neural networks appear more frequently to be involved in explaining neuroscience, and viceversa. In Section IV, we show that the training-with-noise algorithm [13] reproduces the thermodynamics described by Wong and Sherrington in [20, 21]. This implies convergence to a Hebbian matrix [1, 3] or a Support Vector Machine (SVM) [10, 22, 35] when learning random configurations with, respectively, a maximal (i.e. $m_t = 0^+$) and a minimal (i.e. $m_t = 1^-$) amount of noise. The training overlap $m_t \in (0, 1)$ can be then tuned to interpolate between these two models. In Section V, we exploit a novel degree of freedom to access a new path in coupling space. After setting a specific amount of training noise m_t , we constrain the entries of the training configurations to assume a particular internal structure. In the case of maximal noise $m_t = 0^+$, for every training configuration, we define a set of variables ω_i^μ , whose value in the neighborhood of $\Delta_i^\mu = 0$ allows

to infer the classification and generalization power of the training configuration. When this quantity is negative, training drives the network closer to the optimal properties of a SVM.

In this framework, the shape of the initial landscape of attractors where configurations are sampled assumes a crucial role. We find that the Hebbian landscape in the *oblivion* regime (i.e. $\alpha > 0.14$) is a very effective starting condition for learning. Furthermore, our analysis shows that the quality of the configurations, in terms of noise structure, increases when we descend towards the metastable minima of a Hebbian landscape, while the inverse trend is observed in a fully random landscape. In order to reach lower states in the Lyapunov function, we focused on a symmetric version of the training-with-noise algorithm [13]. In particular, we proved that the traditional *unlearning* algorithm [4, 6–8] (see Section III) is recovered from the training-with-noise algorithm (see Section IV) when the noise is maximal and the training configurations are stable fixed points of the dynamics. Therefore, it is now clear that basins of attraction are close to be maximized by the unlearning algorithm [8] because training data are such as to approach the global minimum of the loss function of a SVM. The same principle is traditionally applied by other unsupervised procedures that are similar to unlearning [9, 36, 37]. As a difference with the latter, such algorithms learn configurations that are higher in the landscape of attractors. Consistently with our study, these techniques achieve small or nonexistent basins of attraction, while the traditional unlearning routine, that makes use of the metastable states, approaches an optimal memory performance [8].

The picture about maximally noisy training data is completed by Section VI, where the measure given by the ω_i^μ variables is used to sample efficient training data. Simulations suggest that low saddles favor higher performances even more than stable fixed points do. This result can be exploited to outperform the traditional unlearning algorithm both in terms of critical capacity and basins of attraction.

In addition to the maximal noise scenario, we studied an application of the training-with-noise algorithm when stable fixed points with $m_t > 0$ are learned by the network, when it is initialized according to the Hebb's rule. The resulting algorithm reaches both classification and a good degree of generalization, proving that the internal structure of the configurations plays a relevant role also for higher values of m_t . The critical capacity reached by the algorithm has been numerically estimated.

In light of our work, the full learning and memory consolidation process can be interpreted in terms of a sequential training-with-noise routine in conditions of maximal noise. In the following, we conjecture a new interpretation of learning as it would naturally come from our analysis. During a first *online* phase external stimuli are learned by the network according to the standard training-with-noise algorithm: such stimuli might be conceived to have a very weak overlap with a set of *concepts*

or *archetypes* that should be pseudo-orthogonal with each other and unknowable a-priori. The archetypes are contained in the symmetries and structures of the stimuli. At the end of this phase the initial network, that had been initialized at random, or in the form of a *tabula rasa*, has achieved a Hebbian appearance hiding the unconscious archetypes. The Hebbian network might now be in the non-retrieval regime, hence without any practical utility. A second *offline* phase follows to the first one. Now the network samples structured noisy neural configurations, still weakly correlated with the archetypes, from the freshly formed landscape of attractors. Such states could be, for instance, lower saddles or stable fixed points of the neural dynamics. Consequently, memory is consolidated by centering the unconscious archetypes into very large basins of attraction. From the biological point of view, this picture supports the importance of both daily and night experience in learning, as hebbian learning acquires higher credibility [38, 39] and the role of sleep in consolidating memory has been repeatedly confirmed by electrophysiology [40, 41]. Moreover, the association between the stored memories and pseudo-orthogonal archetypes may present interesting connections with the efforts of early psychopathology to interpret the content of dreams in humans [42]. Most importantly, it should

be noticed that working with maximal noise allows the learning process to go unsupervised, as it is meant to work in real neural networks. Furthermore, learning as composed by two alternating phases is also the object of very recent speculations at the interface between neuroscience and computer science: in analogy with an adversarial network [43, 44], or a Boltzmann Machine [45, 46], the brain would use internal noisy representations to increase the robustness of learning and help generalization. We hope that our results can shed light over the particular structure of noise that is optimal for learning in neural networks, possibly helping to develop a proper theory behind the very empirical techniques of noise injection (i.e. dropout or data augmentation) that are already largely implemented in training deep networks [29, 47, 48] and which can be integrated into a wider concept of memory formation in the brain [49].

ACKNOWLEDGMENTS

The authors are particularly grateful to their mentors Enzo Marinari, Giancarlo Ruocco and Francesco Zamponi for the precious suggestions and support. They also thank Fabian Aguirre Lopez, Aldo Battista, Simona Cocco, Giampaolo Folena, Rémi Monasson and Mauro Pastore for useful discussions.

-
- [1] J.J. Hopfield. Neural networks and physical systems with emergent collective computational abilities. *Proceedings of the National Academy of Sciences*, 79(8):2554, 1982.
 - [2] D.O. Hebb. *The Organization of Behavior : A Neuropsychological Theory*. John Wiley and Sons, 1949.
 - [3] D. J. Amit, H. Gutfreund, and H. Sompolinsky. Storing Infinite Numbers of Patterns in a Spin-Glass Model of Neural Networks. *Physical Review Letters*, 55(14):1530, 1985.
 - [4] J.J. Hopfield, D.I. Feinstein, and R.G. Palmer. ‘Unlearning’ has a stabilizing effect in collective memories. *Nature*, 304(5922):158, 1983.
 - [5] F. Crick and G. Mitchison. The function of dream sleep. *Nature*, 304(5922):111, 1983.
 - [6] J.L. Van Hemmen, L.B. Ioffe, R. Kühn, and M. Vaas. Increasing the efficiency of a neural network through unlearning. *Physica A: Statistical Mechanics and its Applications*, 163(1):386, 1990.
 - [7] J.L. van Hemmen and N. Klemmer. Unlearning and Its Relevance to REM Sleep: Decorrelating Correlated Data. In J.G. Taylor, C.L.T. Mannion, J.G. Taylor, E.R. Caianiello, R.M.J. Cotterill, and J.W. Clark, editors, *Neural Network Dynamics*, page 30. Springer London, London, 1992.
 - [8] M. Benedetti, E. Ventura, E. Marinari, G. Ruocco, and F. Zamponi. Supervised perceptron learning vs unsupervised Hebbian unlearning: Approaching optimal memory retrieval in Hopfield-like networks. *The Journal of Chemical Physics*, 156(10):104107, 2022.
 - [9] S. Wimbauer, N. Klemmer, and J.L. van Hemmen. Universality of unlearning. *Neural Networks*, 7(2):261, 1994.
 - [10] E. Gardner. The space of interactions in neural network models. *Journal of Physics A: Mathematical and General*, 21(1):257, 1988.
 - [11] E. Gardner, H. Gutfreund, and I. Yekutieli. The phase space of interactions in neural networks with definite symmetry. *Journal of Physics A: Mathematical and General*, 22(12):1995, 1989.
 - [12] M. Minsky and P. Seymour. *Perceptrons: an introduction to computational geometry*. MIT Press, 1969.
 - [13] E. J. Gardner, D. J. Wallace, and N. Stroud. Training with noise and the storage of correlated patterns in a neural network model. *Journal of Physics A: Mathematical and General*, 22(12):2019, June 1989.
 - [14] T.B. Kepler and L.F. Abbott. Domains of attraction in neural networks. *Journal de Physique*, 49(10):1657, 1988.
 - [15] E. Gardner. Structure of metastable states in the Hopfield model. *Journal of Physics A: Mathematical and General*, 19(16):L1047, 1986.
 - [16] D.J. Amit. *Modeling Brain Function*. Cambridge University Press, 1989.
 - [17] B.M. Forrest. Content-addressability and learning in neural networks. *Journal of Physics A: Mathematical and General*, 21(1):245, 1988.
 - [18] Y. Le Cun. Learning Process in an Asymmetric Threshold Network. In *Disordered Systems and Biological Organization*, page 233. Springer, Berlin, Heidelberg, 1986.
 - [19] E. Gardner. Optimal basins of attraction in randomly sparse neural network models. *Journal of Physics A: Mathematical and General*, 22(12):1969, 1989.

- [20] K.Y.M. Wong and D. Sherrington. Optimally adapted attractor neural networks in the presence of noise. *Journal of Physics A: Mathematical and General*, 23(20):4659, 1990.
- [21] K.Y.M. Wong and D. Sherrington. Neural networks optimally trained with noisy data. *Physical Review E*, 47(6):4465, 1993.
- [22] B. Schölkopf and A.J. Smola. *Learning with Kernels: Support Vector Machines, Regularization, Optimization, and Beyond*. The MIT Press, 2018.
- [23] B. Derrida, E. Gardner, and A. Zippelius. An Exactly Solvable Asymmetric Neural Network Model. *Europhysics Letters (EPL)*, 4(2):167, 1987.
- [24] M. Newman and G. Barkema. *Monte Carlo Methods in Statistical Physics*. Oxford University Press, 1999.
- [25] D. Sherrington and S. Kirkpatrick. Solvable Model of a Spin-Glass. *Physical Review Letters*, 35(26):1792, 1975.
- [26] G. Pöppel and U. Krey. Dynamical Learning Process for Recognition of Correlated Patterns in Symmetric Spin Glass Models. *Europhysics Letters (EPL)*, 4(9):979, 1987.
- [27] T. Aspelmeier, R.A. Blythe, A.J. Bray, and M.A. Moore. Free energy landscapes, dynamics and the edge of chaos in mean-field models of spin glasses. *Physical Review B*, 74(18):184411, 2006.
- [28] S. Kirkpatrick, C.D. Gelatt, and M.P. Vecchi. Optimization by simulated annealing. *Science*, 220(4598):671, 1983.
- [29] N. Srivastava, G. Hinton, A. Krizhevsky, I. Sutskever, and R. Salakhutdinov. Dropout: A simple way to prevent neural networks from overfitting. *Journal of Machine Learning Research*, 15:1929, 2014.
- [30] T. Tadros, G. Krishnan, R. Ramyaa, and Bazhenov M. Biologically inspired sleep algorithm for increased generalization and adversarial robustness in deep neural networks. *International Conference on Learning Representations*, 2019.
- [31] D. Saad and S. Solla. Learning with Noise and Regularizers in Multilayer Neural Networks. In *Advances in Neural Information Processing Systems*, volume 9. MIT Press, 1996.
- [32] B. Schottky and U. Krey. Phase transitions in the generalization behaviour of multilayer perceptrons: II. The influence of noise. *Journal of Physics A: Mathematical and General*, 30(24):8541, 1997.
- [33] E. Hoel. The overfitted brain: Dreams evolved to assist generalization. *Patterns*, 2(5):100244, 2021.
- [34] F. Stella, P. Baracska, J. O'Neill, and J. Csicsvari. Hippocampal Reactivation of Random Trajectories Resembling Brownian Diffusion. *Neuron*, 102(2):450, 2019.
- [35] S. Diamond and S. Boyd. CVXPY: A Python-Embedded Modeling Language for Convex Optimization. *Journal of Machine Learning Research*, 17:1, 2016.
- [36] K. Nokura. Paramagnetic unlearning in neural network models. *Physical Review E*, 54(5):5571, 1996.
- [37] A.Y. Plakhov and S.A. Semenov. The modified unlearning procedure for enhancing storage capacity in Hopfield network. In *[Proceedings] 1992 RNNS/IEEE Symposium on Neuroinformatics and Neurocomputers*, page 242, Rostov-on-Don, Russia, 1992. IEEE.
- [38] Y. Miyashita, M. Kameyama, I. Hasegawa, and T. Fukushima. Consolidation of Visual Associative Long-Term Memory in the Temporal Cortex of Primates. *Neurobiology of Learning and Memory*, 70(1-2):197, 1998.
- [39] G. Buzsaki. Neural Syntax: Cell Assemblies, Synapses, and Readers. *Neuron*, 68(3):362, 2010.
- [40] J.D. Creery, D.J. Brang, J.D. Arndt, A. Bassard, V.L. Towle, J.X. Tao, S. Wu, S. Rose, P.C. Warnke, N.P. Issa, and K.A. Paller. Electrophysiological markers of memory consolidation in the human brain when memories are reactivated during sleep. *Proceedings of the National Academy of Sciences*, 119(44):e2123430119, 2022.
- [41] N. Maingret, G. Girardeau, R. Todorova, M. Goutierre, and M. Zugaro. Hippocampo-cortical coupling mediates memory consolidation during sleep. *Nature Neuroscience*, 19(7):959, 2016.
- [42] S. Freud. *Die Traumdeutung*. Franz Deuticke, Vienna, 1899.
- [43] N. Deperrois, M.A. Petrovici, W. Senn, and J. Jordan. Learning cortical representations through perturbed and adversarial dreaming, 2022.
- [44] I. Goodfellow, J. Pouget-Abadie, M. Mirza, B. Xu, D. Warde-Farley, S. Ozair, A. Courville, and Y. Bengio. Generative Adversarial Nets. In *Advances in Neural Information Processing Systems*, volume 27. Curran Associates, Inc., 2014.
- [45] G. Hinton. The Forward-Forward Algorithm: Some Preliminary Investigations. *arXiv:2212.13345*, 2022.
- [46] J. Hinton and T.J. Sejnowski. *Unsupervised Learning: Foundations of Neural Computation*. The MIT Press, 1999.
- [47] C. Shorten and T. M. Khoshgoftaar. A survey on Image Data Augmentation for Deep Learning. *Journal of Big Data*, 6(1):1, 2019.
- [48] U.M. Tomasini, L. Petrini, F. Cagnetta, and M. Wyart. How deep convolutional neural networks lose spatial information with training. *arXiv:2210.01506*, 2023.
- [49] L. Bonnasse-Gahot and J.P. Nadal. Categorical Perception: A Groundwork for Deep Learning. *Neural Computation*, 34(2):437, 2022.
- [50] M. Mezard, G. Parisi, and M. Virasoro. *Spin Glass Theory and Beyond: An Introduction to the Replica Method and Its Applications*, volume 9 of *World Scientific Lecture Notes in Physics*. World Scientific, 1986.

Appendix A: Reduction of the \mathcal{L} function

1. Training with noise

At each step of the algorithm a memory label μ_d is sampled at random and the update (8) is performed over the couplings. The new value of the \mathcal{L} function (14) is

$$\mathcal{L}' = -\frac{1}{\alpha N^2} \sum_{i,\mu}^{N,p} \operatorname{erf} \left(\frac{m\Delta_i^\mu}{\sqrt{2(1-m^2)}} + \frac{\lambda m}{N\sigma_i \sqrt{2N(1-m^2)}} \epsilon_i^{\mu_d} \xi_i^\mu \xi_i^{\mu_d} \sum_{j \neq i} S_j^{\mu_d} \xi_j^\mu \right). \quad (\text{A1})$$

Since $\delta\sigma_i \propto \frac{\lambda}{N} \frac{J_i}{\sigma_i} + O\left(\frac{\lambda}{N}\right)^3$ and the mean J_i of the couplings along line i equals zero by initialization and it is naturally maintained null during the algorithm, we have considered $\sigma'_i \simeq \sigma_i$. Then \mathcal{L}' can be rewritten as

$$\begin{aligned} \mathcal{L}' = & -\frac{1}{\alpha N^2} \sum_{i,\mu \neq \mu_d}^{N,p} \operatorname{erf} \left(\frac{m\Delta_i^\mu}{\sqrt{2(1-m^2)}} + O\left(\frac{1}{N}\right) \right) - \\ & - \frac{1}{\alpha N^2} \sum_i^N \operatorname{erf} \left(\frac{m\Delta_i^{\mu_d}}{\sqrt{2(1-m^2)}} + \frac{\lambda m \cdot m_t}{\sigma_i \sqrt{2N(1-m^2)}} \epsilon_i^{\mu_d} + O\left(\frac{1}{N}\right) \right), \quad (\text{A2}) \end{aligned}$$

where we have used that $\frac{1}{N} \sum_{j \neq i} \xi_j^\mu S_j^{\mu_d} = O(N^{-1/2})$ when $\mu \neq \mu_d$ and $m_t = O(1)$. We thus expand the errorfunction at the first order in $O(N^{-1/2})$ obtaining the variations to \mathcal{L} in equation (16).

2. Training with structured noise

The new value of \mathcal{L} is derived by using equation (17) to evaluate the variation of stabilities

$$\begin{aligned} \mathcal{L}' = & -\frac{1}{\alpha N^2} \sum_{i,\mu}^{N,p} \operatorname{erf} \left(\frac{m\Delta_i^\mu}{\sqrt{2(1-m^2)}} + \frac{\lambda m \xi_i^\mu \xi_i^{\mu_d}}{2N\sigma_i \sqrt{2N(1-m^2)}} \sum_{j=1}^N S_j^{\mu_d} \xi_j^\mu + \frac{\lambda m \xi_i^\mu S_i^{\mu_d}}{2N\sigma_i \sqrt{2N(1-m^2)}} \sum_{j=1}^N \xi_j^{\mu_d} \xi_j^\mu - \right. \\ & \left. - \frac{\lambda m \xi_i^\mu S_i^{1,\mu_d}}{2N\sigma_i \sqrt{2N(1-m^2)}} \sum_{j=1}^N S_j^{\mu_d} \xi_j^\mu - \frac{\lambda m \xi_i^\mu S_i^{\mu_d}}{2N\sigma_i \sqrt{2N(1-m^2)}} \sum_{j=1}^N S_j^{1,\mu_d} \xi_j^\mu \right), \quad (\text{A3}) \end{aligned}$$

where $\sigma'_i \simeq \sigma_i$ as in the previous paragraph. We now redefine $\chi_i^\mu = \xi_i^\mu S_i^{\mu_d}$, $\chi_i^{1,\mu} = \xi_i^\mu S_i^{1,\mu_d}$, $m_\mu = \frac{1}{N} \sum_{j=1}^N S_j^{\mu_d} \xi_j^\mu$ and $m_{1,\mu} = \frac{1}{N} \sum_{j=1}^N S_j^{1,\mu_d} \xi_j^\mu$ and expand the errorfunction at the first order in $O(N^{-1/2})$ obtaining

$$\delta\mathcal{L} = \frac{m\lambda}{\sqrt{2\alpha^2 N^5 (1-m^2)}} \sum_{i,\mu}^{N,p} \frac{1}{2\sigma_i} \left[(m_\mu \chi_i^{1,\mu} + m_{1,\mu} \chi_i^\mu) - (m_\mu \xi_i^\mu \xi_i^{\mu_d} + M_\mu^{\mu_d} \chi_i^\mu) \right] \exp \left(-\frac{m^2 \Delta_i^{\mu^2}}{2(1-m^2)} \right) \quad (\text{A4})$$

where $M_\mu^{\mu_d} = \frac{1}{N} \sum_{i=1}^N \xi_i^\mu \xi_i^{\mu_d}$. Equation (A4) can be decomposed in

$$\delta\mathcal{L} = \delta\mathcal{L}_N + \delta\mathcal{L}_U \quad (\text{A5})$$

where $\delta\mathcal{L}_U$ contains the weight

$$\omega_i^\mu = \frac{1}{2\sigma_i} (m_\mu \chi_i^{1,\mu} + m_{1,\mu} \chi_i^\mu) \quad (\text{A6})$$

while $\delta\mathcal{L}_N$ contains

$$\Omega_i^\mu = \frac{1}{2\sigma_i} (m_\mu \xi_i^\mu \xi_i^{\mu_d} + M_\mu^{\mu_d} \chi_i^\mu) \quad (\text{A7})$$

We study the two contributions numerically, on a Hebbian network, i.e. with no learning going on, for the case of $m_t = 0^+$. The Pearson coefficient is measured between the vector of the stabilities Δ_i^μ and the weights ω_i^μ as well

as with Ω_i^μ separately. This quantity should underline an eventual reciprocal dependence between $\omega_i^\mu, \Omega_i^\mu$ and Δ_i^μ . The test is repeated over states sampled by a Monte Carlo at different temperatures T . Results are reported in fig. 17 where it is evident that Ω does not have any correlation with Δ , while the dependence of ω by the stabilities is evident. This aspect holds during the training procedure also, as it can be observed by performing the same measure at different step of the training-with-noise procedure over states with $m_t = 0^+$. We will refer to $\delta\mathcal{L}_U$ as the relevant contribution to the variation of the function \mathcal{L} .

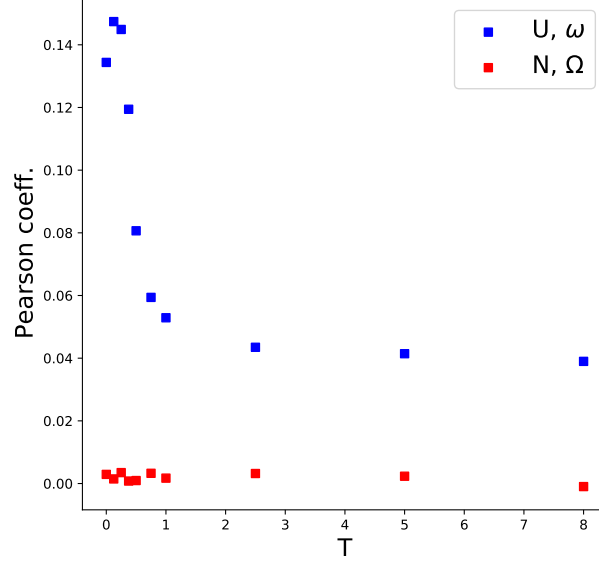


FIG. 17: Pearson coefficient measuring the correlation between $\omega_i^\mu, \Omega_i^\mu$ and the stabilities Δ_i^μ in the case of a Hebbian network at different temperatures T . Configurations at a given temperature T have been sampled by a Monte Carlo of the Kawasaki kind, in order to choose only maximally noisy states ($m_t = 0^+$). Points are collected from 15 samples of the network. Choice of the parameters: $N = 500, \alpha = 0.5$.

Appendix B: Training with noise - computation of n_{SAT}

We now resume the computations performed in [21][20] to explain how the images in Sections (IV A)-(IV B) are made. We restrict ourselves to a spherical space of interactions such that

$$\sum_{j \neq i} J_{ij}^2 - N = 0 \quad \forall i \quad (\text{B1})$$

We want to compute the probability distribution of the stabilities that now become

$$\Delta_i^\mu = \xi_i^\mu \sum_{j=1}^N \frac{J_{ij}}{\sqrt{N}} \xi_j^\mu \quad (\text{B2})$$

The partition function of the model is then given by

$$Z = \int \prod_{i,j} dJ_{ij} \delta \left(\sum_{j \neq i} J_{ij}^2 - N \right) \exp \left(-\beta \mathcal{L}(m_t, J) \right) \quad (\text{B3})$$

where β is the inverse annealing temperature of the problem and the loss function \mathcal{L} is defined in eq. (14). The distribution of the stabilities is

$$\rho_{m_t}(\Delta) = \frac{1}{Z} \int \prod_j dJ_{\bullet j} \delta \left(\sum_j J_{\bullet j}^2 - N \right) \exp \left(\beta \sum_\mu \text{erf} \left(\frac{m_t \xi_\bullet^\mu \sum_j J_{\bullet j} \xi_j^\mu}{\sqrt{2N(1-m_t^2)}} \right) \right) \delta \left(\xi_\bullet^1 \sum_j \frac{J_{\bullet j}}{\sqrt{N}} \xi_j^1 - \Delta \right) \quad (\text{B4})$$

Where $\overline{\cdot}$ denotes the average over the realizations of the memories and we have neglected the factorization over i , since we treat the optimization process as independent along the lines of the J_{ij} matrix. Index i has been nevertheless substituted by \bullet for the sake of completeness. Replicas can be used to evaluate the normalization, i.e.

$$1/Z = \lim_{n \rightarrow 0} Z^{n-1} \quad (\text{B5})$$

The replica calculation in the replica symmetric ansatz [50] when $\beta \rightarrow \infty$ leads to the following expression for $\rho_{m_t}(\Delta)$

$$\rho_{m_t}(\Delta) = \frac{1}{\sqrt{2\pi}} \left(1 + \sqrt{\frac{2}{\pi}} \frac{m_t^3 \chi}{(1 - m_t^2)^{3/2}} \Delta \exp \left(-\frac{m_t^2 \Delta}{2(1 - m_t^2)} \right) \right) \exp -\frac{w(\Delta)^2}{2} \quad (\text{B6})$$

where χ and w are derived by solving the following two equations

$$w = x - \frac{\sqrt{2} m_t \chi}{\sqrt{\pi(1 - m_t^2)}} \exp \left(-\frac{m_t^2 x^2}{2(1 - m_t^2)} \right) \quad (\text{B7})$$

$$\int Dw (x^*(w, \chi) - w)^2 = \alpha^{-1} \quad (\text{B8})$$

with x^* being the solution of (B7) and Dw being the standard Gaussian measure with zero mean and unitary variance. Eventually, the fraction of stable directions in the memories is computed as

$$n_{SAT}(m_t, \alpha) = \int_0^{+\infty} d\Delta \rho_{m_t}(\Delta) \quad (\text{B9})$$

Appendix C: Training with noise - measurement of the basins of attraction

We report here a general experimental procedure to measure the average size of the basins of attraction of a neural network of finite size N and a given choice of the control parameters.

The network is firstly trained according to an algorithm of our choice. Once the couplings have been found the asynchronous version of dynamics (1) is initialized in one of the memories. The dynamics is run until convergence onto the attractor associated to the basin of belonging of the memory. Now the retrieval map $m_f(m_0)$ is measured with respect to that particular attractor and the procedure is repeated over different memories and realizations of the network. The average radius of the basin of attraction is then measured as the value of $1 - m_0$ where $m_f(m_0)$ equals a reference value. In our case such value is $m_f = 0.98$.

We have applied this procedure on networks trained either as SVMs and with the training-with-noise algorithm. In the former case a convex algorithm contained in the *cvxpy* Python domain [35] is implemented to train the SVM. To be more specific, N independent machines are trained to correctly classify $p = \alpha N$ binary memories of the kind of $\vec{\xi}^\mu \in \{-1, +1\}^N$ having as labels ξ_i^μ with $i \in [1, \dots, N]$.

Regarding the dynamics, the stability of fixed points is in general implied by some properties of the couplings, mainly their degree of symmetry. For the case of the training-with-noise algorithm we start from a random symmetric matrix, as done in [14]: the update of the couplings will only perturb the initial symmetry yet allowing the measures to be still consistent with the theory. On the other hand, SVMs are found to be sufficiently symmetric for allowing the asynchronous dynamics to converge. The comparison between the retrieval maps obtained for the two algorithms with $\alpha = 0.45$ and $N = 200$ is reported in fig. 18. The curve relative to the SVM is fixed, while the one associated with the training-with-noise is changing with respect to the training overlap m_t .

Even if the SVM always accomplishes to reach classification for $\alpha < 2$ [10], a network trained with noise might live in two different behaving regimes: the *retrieval* phase of the network, i.e. the regime where the memory is close to the relative attractor, and the *non-retrieval* phase, i.e. the regime where the memory is far from its attractor. In particular network models where couplings are assembled in a supervised fashion from the memories, as in [1] or [], the transition between the two phases can be computed analytically. In the case of training-with-noise this cannot be done. We then advance an empirical criterion to determine the transition between the *retrieval* phase and the *non-retrieval* one. We consider the m_t^* such that

$$\left. \frac{dm_f}{dm_0}(m_t^*) \right|_{m_0=1} = 1 \quad (\text{C1})$$

as the training overlap that signals the passage from the non-retrieval regime to the retrieval one. This condition arose in analogy with the analysis of the one-step retrieval map in [21]. The numerical extrapolation of the overlap in fig. 5 shows a good agreement between the real separation between the two regimes and the line estimated by condition (C1), even at different values of N .

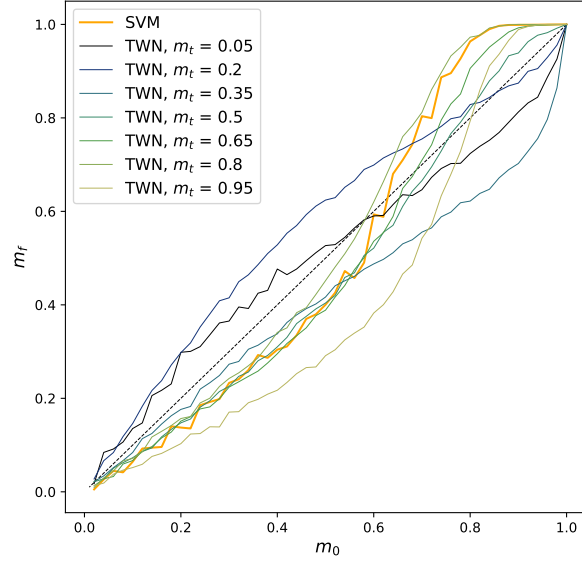


FIG. 18: Retrieval map $m_f(m_0)$ in the case of networks trained through SVM and training-with-noise algorithms. Curves are shown as a function of m_t and compared with the bisector, indicated with a *dashed black* line. Points are averaged over 10 samples. Choice of the parameters: $N = 200$, $\alpha = 0.45$.